Assessment of the effect of process conditions and material characteristics of alkali metal salt-promoted MgO-based sorbents on their CO_2 capture performance

Jian Chen,[†,‡] *Lunbo Duan,*[*,†] *Felix Donat,*[*,‡] *Christoph R. Müller*[*,‡]

[†] Key Laboratory of Energy Thermal Conversion and Control, Ministry of Education, School of Energy and Environment, Southeast University, Nanjing 210096, China

[‡] Laboratory of Energy Science and Engineering, Department of Mechanical and Process Engineering, ETH Zürich, Leonhardstrasse 21, 8092 Zürich, Switzerland

Email: duanlunbo@seu.edu.cn; donatf@ethz.ch; muelchri@ethz.ch

ABSTRACT: CO_2 capture using alkali metal salt (AMS)-promoted MgO-based sorbents at intermediate temperatures (300 – 500 °C) has gained increased interest recently. The prospects of such materials for CO_2 capture were assessed in this work. We investigated the most reactive MgO-based sorbents that have been reported in the literature, i.e., MgO promoted with a combination of various AMS (incl. $NaNO_3$, $LiNO_3$, K_2CO_3 and Na_2CO_3), and examined how particle size (from powder to pelletized 500 μm particles) and reaction conditions (calcination/carbonation

temperature, and partial pressure of CO_2) affect the cyclic CO_2 uptake using a thermogravimetric analyzer (TGA) at ambient pressure. The TGA results showed that the CO_2 uptake of the sorbents decreased significantly after pelletization, losing 74 % of its initial capacity. However, the CO_2 uptake capacity of the pelletized sorbents continued to increase over 100 cycles and reached a value (~ 0.46 $g_{CO2}/g_{sorbent}$) close to that of the powdery sample (~ 0.53 $g_{CO2}/g_{sorbent}$). Analysis via X-ray diffraction (XRD), inductively coupled plasma optical emission spectroscopy (ICP-OES), scanning electron microscope (SEM) and N_2 physisorption suggests that the increase in CO_2 uptake was related to a change of the nature of the alkali species within the molten phase that is reflected by their re-crystallization behavior when cooling them down to room temperature, and appeared to be affected by the CO_2 partial pressure present during carbonation. Finally, the CO_2 capture performance of the best-performing sorbents was evaluated in a packed bed reactor, in order to assess whether the most reactive sorbents are capable of removing a significant amount of CO_2 from a gas stream at ambient pressure. The CO_2 uptake of the sorbents in the packed bed experiments was very close to that in the TGA experiments; however, the CO_2 capture efficiency was less than 10 %, which currently appears too low for an industrial post-combustion CO_2 capture process to be viable. New material developments should not only focus on improving the rate of formation of $MgCO_3$ from MgO, but also assess whether CO_2 removal with such sorbents is actually feasible.

KEYWORDS: CO_2 capture, MgO-based sorbents, alkali metal salt, CO_2 partial pressure, CO_2 capture efficiency

INTRODUCTION

CO_2 capture and storage (CCS) is an important part of the strategies to reduce anthropogenic CO_2 emissions and mitigate climate change. The most expensive part of the CCS steps CO_2 capture, transport and storage, is the capture part, and substantial efforts have been devoted to developing effective and economically feasible CO_2 capture technologies.[1–3] Amongst them, the CO_2 capture using MgO-based sorbents via a reversible carbonation/calcination reaction ($MgO + CO_2 \leftrightarrow MgCO_3$) at intermediate temperatures (300 – 500 °C) has gained increased interest recently.[4,5] MgO-based sorbents exhibit promising prospects due to their wide availability, low cost, non-toxicity, and high theoretical CO_2 uptake capacity (~ 1.1 g CO_2 per g MgO). CO_2 captured by MgO-based sorbents can be released at relatively low temperatures in a less endothermic reaction compared to other solid sorbents that are commonly used, such as CaO-based sorbents; the calcination temperatures range from ~ 400 – 500 °C for MgO-based sorbents compared to 850 – 950 °C for CaO-based sorbents.[6–8] However, using bulk MgO as the sorbent for CO_2 capture is challenging owing to its poor sorption kinetics, resulting in a fairly low effective CO_2 uptake capacity (~ less than 0.01 $g_{CO2}/g_{sorbent}$ after 60 min at 400 °C in pure CO_2[9]) that limits its potential use in industrial applications.

Extensive studies have been conducted to improve the CO_2 uptake capacity and stability of MgO-based sorbents, including optimization of the reaction temperatures,[10,11] the synthesis of highly porous MgO with specific surface areas > 200 m^2/g,[12–14] the incorporation of structural stabilizers,[15–17] and the doping with alkali metal salt (AMS).[4,5,18] The doping of MgO with AMS is considered the most effective approach; it is also relatively inexpensive and potentially suitable for large-scale production. A wide range of single AMS or a combination of various AMS (typically alkali nitrates and/or carbonates) has been used to modify MgO-based sorbents, with the main results of some selected studies summarized in Table 1. The AMS (or mixtures thereof) is

able to partially dissolve bulk MgO and to overcome the high lattice energy constraints, resulting in a much higher and more cyclically stable CO_2 capture performance compared to bulk MgO.[19,20] Another important parameter to enable fast CO_2 sorption is the solubility and transport of the CO_2 within the AMS.[21,22]

Table 1. Summary of the CO_2 capture performance of the AMS-promoted MgO-based sorbents reported previously and in this work.

Alkali metal salt(s)	Temperature (°C)/Atmosphere/Time (min)		Cycles	CO_2 uptake ($g_{CO2}/g_{sorbent}$)		Ref.
	Calcination	Carbonation		Initial	Final	
$NaNO_3$	300/He/180	300/10 vol.% CO_2/180	5	0.39	0.21	22
$NaNO_3$	450/N_2/60	300/CO_2/180	8	0.12	0.31	23
$NaNO_3$	400/N_2/60	330/CO_2/60	15	0.22	0.37	24
$NaNO_3$	450/N_2/30	300/CO_2/30	20	0.14	0.10	25
$NaNO_2$	400/N_2/10	300/CO_2/60	10	0.55	0.29	26
KNO_3	450/N_2/30	325/CO_2/20	12	0.10	0.08	27
(Li, K)NO_3	500/N_2/10	350/CO_2/60	14	0.45	0.34	28
$NaNO_3$-Na_2CO_3	450/N_2/10	325/CO_2/60	14	0.30	0.32	29
$NaNO_3$-$NaNO_2$	400/N_2/20	350/85 vol.% CO_2/60	15	0.83	0.38	30
$NaNO_3$-Na_2CO_3	400/N_2/40	360/CO_2/80	30	0.71	0.25	31
(Li, Na, K)NO_3	450/N_2/15	300/CO_2/60	10	0.48	0.35	32
(Li, Na, K)NO_3	400/N_2/30	300/CO_2/30	20	0.36	0.14	33
(Li, Na, K)NO_3	500/N_2/10	300/CO_2/30	20	0.32	0.16	34
(Li, Na, K)NO_3	350/N_2/30	300/CO_2/60	40	0.27	0.30	35
(Li, Na)NO_3-Na_2CO_3	400/N_2/5	325/CO_2/30	30	0.44	0.29	36
(Li, Na)NO_3-Na_2CO_3	425/N_2/15	325/CO_2/60	30	0.50	0.45	37
(Li, K)NO_3-(Na, K)$_2CO_3$	400/N_2/15	350/40 vol.% CO_2/60	20	0.67	0.52	38
(Li, K)NO_3-(Na, K)$_2CO_3$	450/N_2/90	325/CO_2/180	30	0.84	0.69	39
(Li, K)NO_3-(Na, K)$_2CO_3$	420/N_2/10	350/50 vol.% CO_2/30	30	0.56	0.56	40
(Li, K)NO_3-(Na, K)$_2CO_3$	400/N_2/15	350/CO_2/45	50	0.57	0.57	41
(Li, K)NO_3-(Na, K)$_2CO_3$[a]	400/N_2/15	350/80 vol.% CO_2/30	100	0.35	0.53	this work
(Li, K)NO_3-(Na, K)$_2CO_3$[b]	400/N_2/15	350/80 vol.% CO_2/30	100	0.18	0.46	this work

a: AMS-MgO-1-PO (powder).

b: AMS-MgO-1-PE sieved to 106 – 180 μm.

However, the majority of the studies dealing with AMS-promoted MgO-based sorbents have investigated only their cyclic performance using different combinations of AMS and have determined the CO_2 uptake (and release) in thermogravimetric analyzers (TGA). Moreover, powdery MgO-based sorbents[19-39] and/or high CO_2 concentrations with long durations during the carbonation stage have commonly been used in these studies (Table 1), which may not reflect practically relevant reaction conditions. The potential of MgO-based sorbents for industrial applications (both pre- and post-combustion CO_2 capture) can only be assessed if realistic CO_2 concentrations and sorption times are employed. To the best of our knowledge, such work has not been conducted thus far for the potential application of these materials in post-combustion CO_2 capture.

Herein, we assess the prospects of MgO-based sorbents for post-combustion CO_2 capture at ambient pressure and provide a detailed analysis on the physical and chemical transformation of the sorbents during cycling. We investigate the most reactive MgO-based sorbents that have been reported in the literature,[38–41] i.e., MgO promoted with a combination of various AMS (incl. $LiNO_3$, KNO_3, Na_2CO_3, and K_2CO_3) as shown in Table 1, and show how the particle size (from powder to pelletized 500 μm particles) and the reaction conditions (i.e., carbonation/calcination temperature and partial pressure of CO_2 in carbonation and calcination reactions) affect the cyclic performance using a TGA at ambient pressure. The observed performance of the sorbents is correlated with morphological (pore volume and surface area) and structural changes (the composition of crystalline phases and the transformation of the AMS) over 100 cycles. In addition, we investigate in packed bed experiments with a long gas-solid contact time whether the most reactive sorbents (i.e., those with a CO_2 uptake capacity of ~ 0.46 $g_{CO2}/g_{sorbent}$ after only 30 min)

are actually capable of removing a significant amount of CO_2 from a gas stream – the main purpose of any CO_2 capture technique.

EXPERIMENTAL SECTION

Materials and sorbent preparation

The synthesis approach of AMS-promoted MgO-based sorbents developed by Cui et al.[41] was used and modified in this work. First, $MgCO_3$ (Acros Organics) was calcined in stagnant air at 450 °C in a muffle furnace for 1 h to yield MgO (using a heating rate of 3 °C/min). Subsequently, 2.93 g calcium D-gluconate monohydrate (Sigma-Aldrich) was mixed with 5 g calcined MgO in ethanol (100 mL) under stirring at room temperature for 1 h to give a Ca/Mg molar ratio of 5:95, followed by drying at 80 °C in an oven overnight. After drying, the resulting white powder was calcined at 600 °C in a muffle furnace for 2 h using a heating rate of 3 °C/min. The resulting material is denoted as Mg95Ca5.

The actual AMS-promoted MgO-based sorbents were prepared by the wet mixing of Mg95Ca5 and a mixture of alkali metal salts in ethanol (100 mL) under stirring at room temperature for 3 h. The mixture of alkali metal salts used here contained $LiNO_3$ (Sigma-Aldrich), KNO_3 (Sigma-Aldrich), Na_2CO_3 (Acros Organics) and K_2CO_3 (Fisher Scientific). Different from using a fixed ratio (~ 2:1) as reported in the literature,[41] three molar ratios of (Li, K)NO_3 to (Na, K)$_2CO_3$ (i.e., 2:1, 1:1 and 1:2) were used. The molar ratios of $LiNO_3$ to KNO_3 and Na_2CO_3 to K_2CO_3, and the molar ratio of the mixture of AMS to Mg95Ca5 were always kept at 0.44:0.56, 0.5:0.5 and 0.16:1, respectively. The weight fractions of the AMS in the sorbents were 27 %, 28 % and 29 %, respectively, when the molar ratios of (Li, K)NO_3 to (Na, K)$_2CO_3$ were 2:1, 1:1 and 1:2.

After stirring, the mixed solution was dried at 80 °C in an oven overnight, followed by calcination in a muffle furnace in stagnant air at 500 °C for 2 h using a heating rate of 3 °C/min.

After calcination, the resultant powdery samples were pelletized at a pressure of 520 MPa by using a manual hydraulic press (Atlas 15T Manual Hydraulic Press, Specac). Finally, the cylindrical pellets were crushed in an agate mortar and sieved to obtain AMS-promoted MgO based-sorbents of different particle sizes (106 – 180 μm, 180 – 250 μm, 250 – 355 μm and 355 – 500 μm).

For simplicity, AMS-MgO-x-PE denotes the pelletized AMS-promoted MgO-based sorbents, where x means the molar ratio of (Li, K)NO_3 to (Na, K)$_2CO_3$ (i.e., 0.5, 1 or 2). In addition, AMS-MgO-x-PO describes the powdery AMS-promoted MgO-based sorbents that were not pelletized and had a particle size < 50 μm. AMS-MgO-1-PO-Ref describes the AMS-MgO-1-PO without the addition of calcium in the material synthesis process. As shown in Figure S1 in the Supporting Information (SI), the addition of calcium in the sorbent increased the CO_2 sorption rate only during the initial cycles, leading to a higher CO_2 uptake capacity, but did not affect significantly the CO_2 capture performance from the seventh cycle onwards.

Sorbent characterization

The chemical composition of the sorbents was investigated using a PANalytical Empyrean X-ray powder diffractometer (XRD). The diffractometer was equipped with an X'Celerator Scientific ultra-fast line detector and Bragg-Brentano HD incident beam optics using Cu Kα radiation (45 kV, 40 mA). Measurements were made in the 2θ range of 10 – 90 ° at a step size of 0.025 ° and a step duration of 0.8 s. The codes of the reference patterns were obtained from the International Centre for Diffraction Data (ICDD). The MgO crystallite size (D) was estimated

using the Scherrer equation ($D = K\lambda/(\beta\cos\theta)$),[42] where K is the shape factor (0.9 assuming a nearly spherical particle), λ is the wavelength of the X-ray radiation used (0.15406 nm), β is the full width at half maximum intensity, and θ is the Bragg angle (peak position) of the corresponding reflection.

The melting points of the AMS mixture were determined from the measured heatflow signals using a TGA with an SDTA sensor (Mettler Toledo TGA/DSC 1). Typically, ~ 30 mg of sample was loaded in a platinum crucible (70 μL), and then heated from room temperature to 500 °C in N_2 using a heating rate of 10 °C/min. The total gas flow rate was 100 mL/min, including a constant N_2 purge gas flow of 25 mL/min to protect the microbalance. All flow rates reported in this work were measured and controlled at ambient temperature and pressure via mass flow controllers (Bronkhorst, EL-Flow).

N_2 physisorption experiments were performed using a NOVA 4000e analyzer (Quantachrome Instruments) at -196 °C. Before the experiment, the samples were degassed under vacuum at 300 °C for 4 h. The surface area and pore volume were determined by the Brunauer-Emmett-Teller (BET) and the Barrett-Joyner-Halenda (BJH) models, respectively.

Elemental analysis of the samples was performed by inductively coupled plasma optical emission spectroscopy (ICP-OES, Agilent 5100 VDV). Furthermore, a high-resolution scanning electron microscope (SEM, FEI Magellan 400) was used to investigate the morphologies of the materials. Before imaging, the samples were sputter-coated (CCU-010 Metal Sputter Coater Safematic) with Pt/Pd to improve their conductivity.

Cyclic CO_2 capture performance

The cyclic CO_2 capture performance of the sorbents was assessed using a TGA (Mettler Toledo TGA/DSC 1) and a packed bed reactor, respectively, both operated at ambient pressure. In

the TGA, the gas-solid contact efficiency is very low, and so most of the CO_2 entering the reaction chamber bypasses the sorbent. In the packed reactor, all of the CO_2 entering the reactor is in contact with the sorbent particles and can potentially be absorbed (subject to the reactivity of the sorbent and the gas-solid contact time).

In the TGA experiments, ~ 20 mg of sample was loaded in a platinum crucible (70 μL) and pre-calcined at 400 °C in N_2 for 30 min. Then, the carbonation reaction was performed at a temperature ranging from 300 – 375 °C in an atmosphere of 15 – 80 vol.% CO_2 (N_2 balance) for 30 min, while the calcination reaction was conducted at a temperature ranging from 400 – 450 °C in N_2 for 15 min, or at 500 °C in 80 vol.% CO_2 (N_2 balance) for 10 min. The carbonation and calcination reactions were repeated for a specified number (up to 100 times). Both the heating and cooling rates were 10 °C/min, respectively. The total gas flow rate was 175 mL/min in each stage, including a constant N_2 purge gas flow of 25 mL/min to protect the microbalance.

In the packed bed experiments, ~ 300 mg of the sample (AMS-MgO-1-PO or AMS-MgO-1-PE sieved to 106 – 180 μm), mixed with 900 mg of SiC (250 – 355 μm), was loaded in a quartz tube (outer diameter: 10 mm, wall thickness: 1 mm), which was then placed inside a vertical tube furnace (Watlow, 350 W, inner diameter: 13 mm). Details of the experimental setup are described in our previous work.[43] Typically, the sample was pre-calcined at 400 °C in N_2 for 30 min. The carbonation reaction was conducted at 325 or 350 °C in an atmosphere of 80 vol.% CO_2 (N_2 balance) for 30 min, while the calcination reaction was conducted at 400 °C in N_2 for 30 min. The carbonation and calcination reactions were repeated eight times. Heating and cooling rates were 100 °C/min and 10 °C/min, respectively. The total gas flow rate was 50 mL/min in each stage. The CO_2 concentration in the off-gas from the packed bed reactor was measured every second by a flue

gas analyzer (ABB, EL3020). The setup was optimized to enable a fast transition between two gas environments.

The CO_2 uptake capacity (in $g_{CO2}/g_{sorbent}$) was used to characterize the CO_2 capture performance of the AMS-promoted MgO-based sorbents. Equations (1) and (2) were used to calculate the observed CO_2 uptake capacity in the TGA and the packed bed experiments, respectively. Equation (3) was used to calculate the CO_2 capture efficiency in the packed bed experiments.

$$\mathrm{CO_2\ uptake\ capacity} = \frac{m_{N,car} - m_{N,cal}}{m_0} \tag{1}$$

$$\mathrm{CO_2\ uptake\ capacity} = \frac{\int_0^t \left(c_{CO_2}^{in} - c_{CO_2}^{out}(t)\right) \mathrm{d}t \cdot Q \cdot M_{CO_2}}{22.4 \cdot m} \tag{2}$$

$$\mathrm{CO_2\ capture\ efficiency} = \frac{\int_0^t \left(c_{CO_2}^{in} - c_{CO_2}^{out}(t)\right) \mathrm{d}t \cdot Q}{Q_{\mathrm{CO_2}} \cdot t} \tag{3}$$

In Equation (1), m_0 (in g) is the mass of the sample after the initial calcination at 400 °C, $m_{N,\mathrm{car}}$ and $m_{N,\mathrm{cal}}$ (in g) represent the mass of the sample after the N^{th} carbonation and calcination reactions, respectively. In Equation (2), m (in g) is the mass of the sample before the experiment, $c_{CO_2}^{in}$ (in %) represents the CO_2 inlet concentration, $c_{CO_2}^{out}(t)$ (in %) denotes the CO_2 outlet concentration at time t, t (in s) is the carbonation time, Q (in L/s) is the total gas flow rate, and M_{CO2} (in g/mol) is the molar mass of CO_2. The divisor 22.4 (in L/mol) is the standard molar volume, which was used to convert the volumetric flow rate into a molar flow rate. The CO_2 uptake capacity was calculated by Equation (2) for the carbonation stage, and there was no significant difference when the CO_2

uptake capacity was instead calculated based on the amount of CO_2 released during the calcination stage. In Equation (3), Q_{CO2} (in L/s) is the CO_2 gas flow rate entering the reactor.

RESULTS AND DISCUSSION

Effect of the calcination/carbonation temperature and the particle size

It is widely accepted that reaction conditions play an important role when investigating materials in gas-solid reactions.[44,45] Based on their thermodynamic properties, MgO-based sorbents have been used for CO_2 capture at intermediate temperatures ranging from 300 to 500 °C (or even lower temperatures when the CO_2 was adsorbed on the surface, rather than being converted into a carbonate). Therefore, the CO_2 capture performance of AMS-promoted MgO-based sorbents was assessed over this temperature range to identify the optimum reaction conditions. Figure 1 shows the cyclic CO_2 uptake of AMS-MgO-2-PE (i.e., the sorbent that had the same composition as the material reported by Cui et al.[41]) sieved to 106 – 180 μm at different carbonation/calcination temperatures. The measured CO_2 uptake capacity increased slightly when the carbonation temperature was increased from 325 to 350 °C (Figures 1a, b), but a further increase in carbonation temperature to 375 °C inhibited the CO_2 capture performance and led to a decrease in the observed CO_2 uptake capacity. This was most likely related to the thermodynamic properties of the MgO-$MgCO_3$ system, and with increasing carbonation temperature at a constant CO_2 concentration, the thermodynamic driving force for the carbonation reaction $MgO + CO_2 \rightarrow MgCO_3$ decreases. Moreover, the CO_2 uptake capacity of the pelletized sorbent decreased with increasing calcination temperature, as is shown in Figures 1c, d, which can be ascribed to the sintering of the sorbent (in particular the $MgCO_3$) at the higher calcination temperature. Thus, the optimal combination of carbonation/calcination temperature was

350/400 °C for the AMS-MgO-2-PE investigated in this work. An extended cycling experiment over 20 cycles was conducted for the AMS-MgO-2-PE sieved to 106 – 180 μm under the optimal reaction conditions, as shown in Figure S2. It is interesting to observe that the pelletized sorbent exhibited a continuously increasing CO_2 uptake capacity over 20 cycles, which is discussed in detail in the following section.

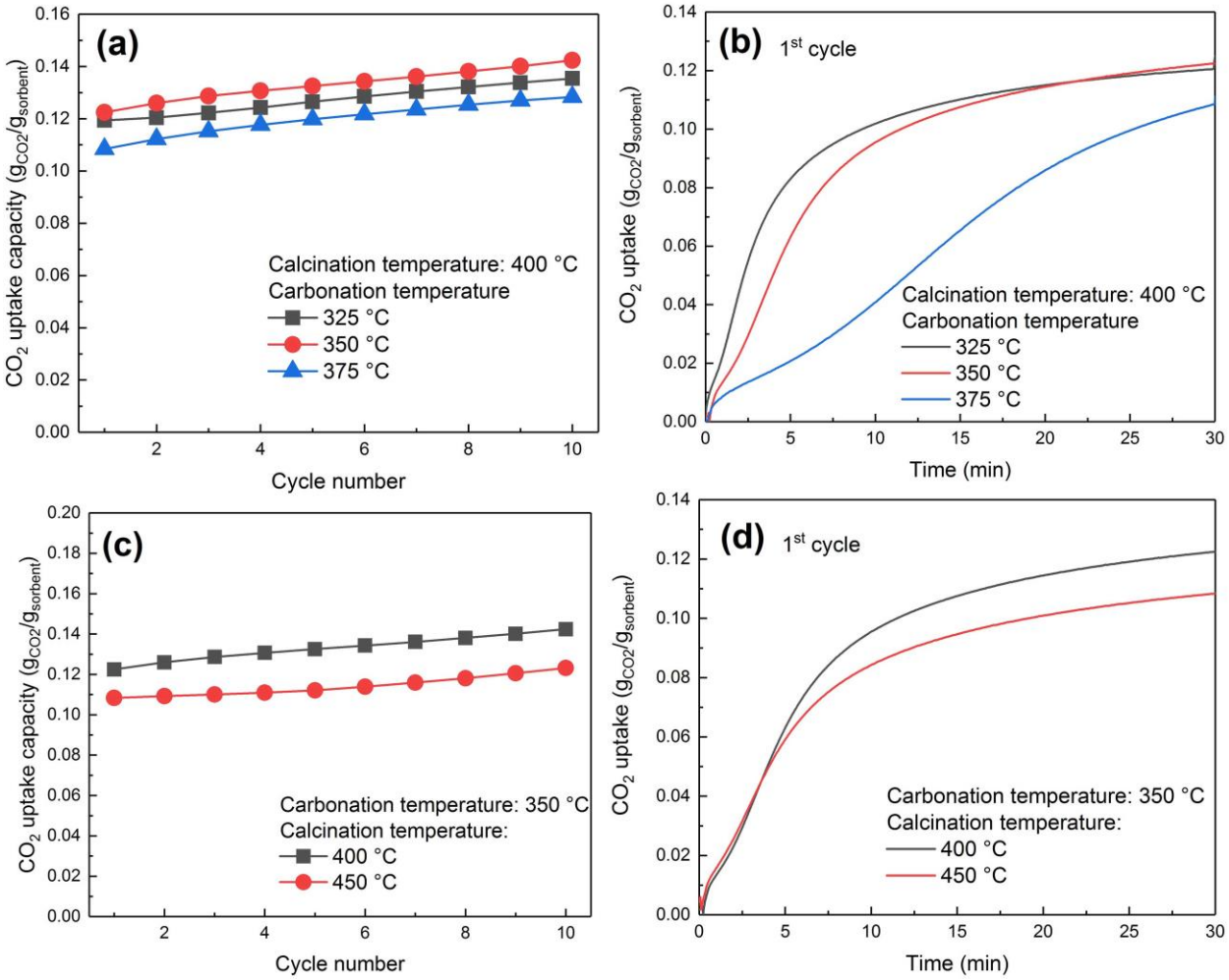

Figure 1. CO_2 capture performance of AMS-MgO-2-PE sieved to 106 – 180 μm at different carbonation and calcination temperatures in the TGA. CO_2 uptake capacity as a function of cycle number at different (a) carbonation and (c) calcination temperatures, and CO_2 uptake as a function

of reaction time at different (b) carbonation and (d) calcination temperatures in the first cycle. Reaction conditions: carbonation: 80 vol.% CO_2 (N_2 bal.), 30 min; calcination: N_2, 15 min.

For potential industrial applications of MgO-based sorbents in packed bed or fluidized bed reactors, it is of practical significance to use sorbents of a certain particle size, but not in powdery form (< 50 μm). However, only few studies have investigated how the particle sizes affect the physical properties and cyclic performance of the sorbents. There are three main techniques to fabricate particles from fine powders at the gram scale, i.e., granulation[46], extrusion[47], or pelletization.[48] In this work, a pelletization method using a manual hydraulic press, was employed to prepare AMS-promoted MgO-based sorbents of different particle sizes (106 – 180 μm, 180 – 250 μm, 250 – 355 μm and 355 – 500 μm). After pelletization, a significant reduction in the surface area of the sorbents was observed (~ 40 %), while only a marginal change in pore volume was observed, as shown in Table 2. With the variation of the particle size, the surface area and pore volume did not differ much as expected, because the different particle size fractions originated from the crushing of the same pellets.

Table 2. Textural properties of the as-synthesized AMS-promoted MgO-based sorbents.

Sample	Surface area (m^2/g)	Pore volume (cm^3/g)
AMS-MgO-0.5-PO	13.3	0.083
AMS-MgO-1-PO	9.5	0.052
AMS-MgO-2-PO	12.1	0.048
AMS-MgO-0.5-PE sieved to 106 – 180 μm	12.4	0.068
AMS-MgO-1-PE sieved to 106 – 180 μm	7.3	0.051
AMS-MgO-2-PE sieved to 106 – 180 μm	8.0	0.041
AMS-MgO-2-PE sieved to 180 – 250 μm	8.0	0.050
AMS-MgO-2-PE sieved to 250 – 355 μm	7.6	0.050
AMS-MgO-2-PE sieved to 355 – 500 μm	7.8	0.050

The CO_2 capture performance of the sorbents sieved to different particle sizes is compared in Figure 2. Both the CO_2 uptake capacity and sorption rate of the sorbents decreased significantly

after pelletization (e.g., in the first cycle from 0.46 $g_{CO2}/g_{sorbent}$ for the powdery sample to 0.12 $g_{CO2}/g_{sorbent}$ for the sample sieved to 106 – 180 μm), which is related to the significant reduction in the surface area and increased diffusional resistance within the particles (Table 2). However, with an increase in particle size, the CO_2 uptake capacity of the sorbents decreased, in absolute terms, only slightly (from 0.12 $g_{CO2}/g_{sorbent}$ for sample sieved to 106 – 180 μm to 0.07 $g_{CO2}/g_{sorbent}$ for sample sieved to 355 – 500 μm), which was due to their similar surface areas and pore volumes. Moreover, all the sorbents exhibited a stable CO_2 uptake capacity over ten cycles.

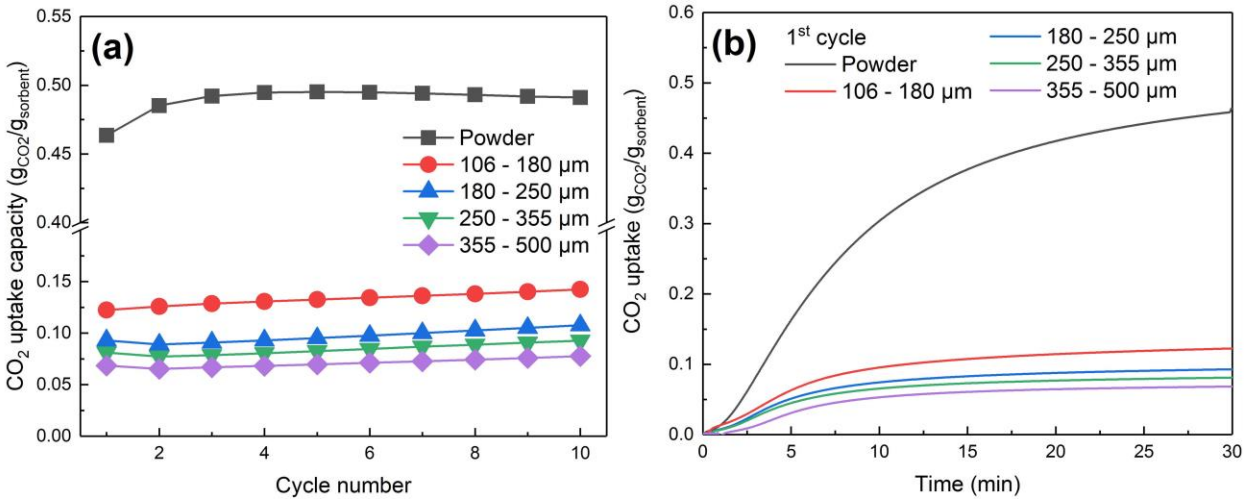

Figure 2. CO_2 capture performance of AMS-MgO-2-PO and AMS-MgO-2-PE sieved to different particle sizes in the TGA. (a) CO_2 uptake capacity as a function of cycle number, and (b) CO_2 uptake as a function of reaction time in the first cycle. Reaction conditions: carbonation: 350 °C, 80 vol.% CO_2 (N_2 bal.), 30 min; calcination: 400 °C, N_2, 15 min.

Effect of molar ratios of (Li, K)NO_3 to (Na, K)$_2CO_3$ in the material

It has been reported that the molar ratio of alkali nitrate to alkali carbonate in MgO-based sorbents plays a critical role in the CO_2 capture performance, because each AMS mixture possesses different physical properties.[38] Thus, we synthesized AMS-promoted MgO-based sorbents with

different molar ratios of (Li, K)NO_3 to (Na, K)$_2CO_3$ (i.e., 2, 1 and 0.5), and then investigated its effect on the CO_2 capture performance. From XRD measurements, changes in the molar ratio of (Li, K)NO_3 to (Na, K)$_2CO_3$ led to slight differences in the chemical compositions (Figure 3a). All as-synthesized sorbents showed XRD peaks due to MgO, $CaCO_3$, K_2CO_3, Na_2CO_3, and KNO_3, but with different relative intensities. No reflections corresponding to $LiNO_3$ were observed, suggesting $LiNO_3$ existed in an amorphous phase. As shown in Figure 3b, the CO_2 capture performance of the sorbents differed significantly, including both the initial CO_2 uptake capacity and the cyclic performance. When the molar ratio of (Li, K)NO_3 to (Na, K)$_2CO_3$ decreased from 2 to 1, the initial CO_2 uptake increased from 0.12 to 0.17 $g_{CO2}/g_{sorbent}$. However, with a further decrease of the molar ratio of (Li, K)NO_3 to (Na, K)$_2CO_3$ to 0.5, the initial CO_2 uptake decreased again, exhibiting a similar CO_2 uptake as the sample with a molar ratio of (Li, K)NO_3 to (Na, K)$_2CO_3$ of 2. It is interesting to observe that the measured CO_2 uptake capacity of the sorbents increased continuously over 15 cycles when the molar ratio of (Li, K)NO_3 to (Na, K)$_2CO_3$ was 1, exceeding its initial capacity by 60 %. In contrast, for the samples with molar ratios of (Li, K)NO_3 to (Na, K)$_2CO_3$ of 2 or 0.5, the CO_2 uptake increased only marginally with cycling, and for a ratio of 0.5 even decreased again after four cycles. The continuous increase in the CO_2 uptake during cycling was also observed for pelletized sorbents sieved to a larger particle size fraction (355 – 500 μm) when the molar ratio of (Li, K)NO_3 to (Na, K)$_2CO_3$ was 1 (Figure 3c). Moreover, the optimal carbonation/calcination temperature of AMS-promoted MgO-based sorbents also changed with the variation of the molar ratio of (Li, K)NO_3 to (Na, K)$_2CO_3$ in the sorbent, as shown in Figure 1 and Figure S3. The optimal combination of carbonation/calcination temperature for both AMS-MgO-2-PE and AMS-MgO-1-PE was 350/400 °C, while the corresponding combination for AMS-MgO-0.5-PE was 325/400 °C. However, note that the optimal reaction

conditions was likely to change after the pelletization. For example, as is shown in Figure S4, the CO_2 uptake capacity of AMS-MgO-1-PO at carbonation temperature of 325 °C was higher than that at 350 °C. Furthermore, the molar ratio of (Li, K)NO_3 to (Na, K)$_2CO_3$ in the sorbent affected its textural properties. AMS-MgO-1-PE sieved to 106 – 180 μm exhibited the highest initial CO_2 uptake, although it had the lowest surface area and pore volume (Table 2). This indicates that the CO_2 uptake capacity of the AMS-promoted MgO-based sorbents was not directly proportional to their textural properties (i.e., surface area and pore volume), which agrees well with the observations made by Wang et al.[38] and Rekhtina et al.[49] The following analyses deal with the AMS-MgO-1-PE and AMS-MgO-1-PO sorbents, which had the optimum ratio of (Li, K)NO_3 to (Na, K)$_2CO_3$ of 1 for the conditions investigated in this work.

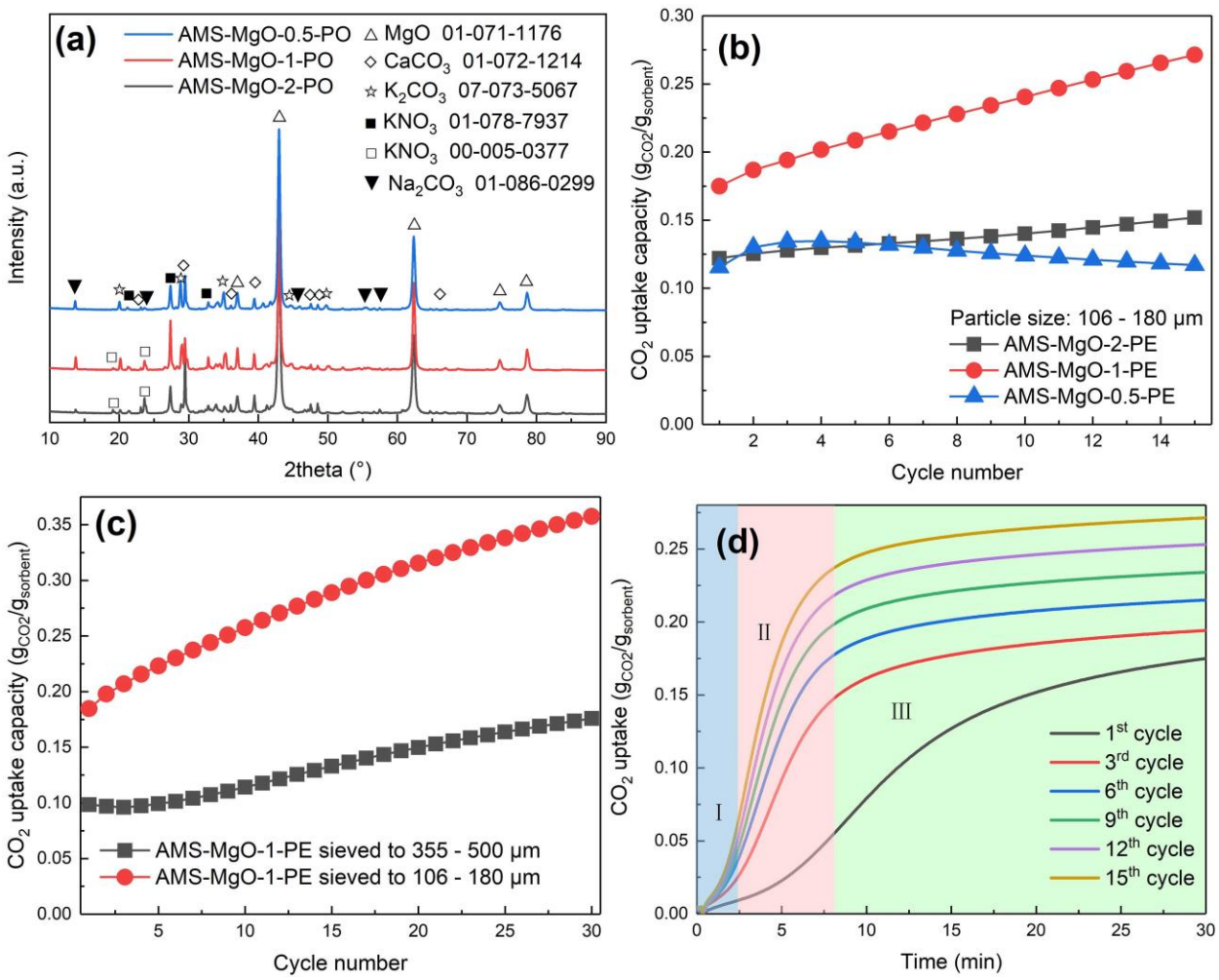

Figure 3. Chemical compositions and CO_2 capture performance of AMS-promoted MgO-based sorbents in the TGA. (a) XRD patterns of the as-synthesized AMS-promoted MgO-based sorbents with different molar ratios of (Li, K)NO_3/(Na, K)$_2CO_3$, (b) CO_2 uptake capacity of pelletized AMS-promoted MgO-based sorbents with different molar ratios of (Li, K)NO_3/(Na, K)$_2CO_3$ as a function of cycle number, (c) CO_2 uptake capacity of AMS-MgO-1-PE sieved to different particle sizes as a function of cycle number, and (d) CO_2 uptake of AMS-MgO-1-PE as a function of reaction time at different cycles. Reaction conditions: carbonation: 350 °C, 80 vol.% CO_2 (N_2 bal.), 30 min; calcination: 400 °C, N_2, 15 min. The blue area represents stage I, the pink area denotes stage II, and the green area means stage III.

Figure 3d shows the CO_2 uptake of the AMS-MgO-1-PE as a function of reaction time at different cycles. From the sigmoidal curve, the carbonation process can be divided into three principal stages. Stage I is an induction period ($0 < t < 2.5$ min), which has been reported previously for MgO-based CO_2 sorbents.[22,34,35,39] The duration of the induction period differs significantly in the different works, and it is affected by many parameters such as the types and the weight fractions of the AMS.[22] However, the reason for such an induction period remains unclear thus far. Harada et al.[35] hypothesized that within this stage, CO_2 is dissolved in the molten AMS coated on the MgO, and then reacts with Mg^{2+} and O^{2-} to form $MgCO_3$. Once the concentration of the CO_2 dissolved in the molten AMS reaches a critical value, CO_2 sorption occurs at a substantially faster rate (stage II, $2.5 < t < 8$ min). Here, nucleation and nuclei-growth of $MgCO_3$ are dominating.[22] Finally, with the progress of the carbonation reaction, the formation of the $MgCO_3$ product layer becomes significant,[34] leading to a decrease in the CO_2 sorption rate (stage III, $t > 8$ min).

Comparisons of the long cyclic performance between the pelletized and powdery AMS-promoted MgO-based sorbents

As shown in Figure 2, the CO_2 uptake capacity of the AMS-promoted MgO-based sorbents was much lower after the sorbents had been pelletized. However, it is surprising to find that the CO_2 uptake capacity of the pelletized sorbents (e.g., AMS-MgO-1-PE sieved to 106 – 180 μm) increased continuously over the first 15 cycles (Figure 3a), and gradually approached the CO_2 uptake capacity of the powdery sorbents. Thus, an extended cycling experiment over 100 cycles was conducted for both pelletized and powdery sorbents, i.e., AMS-MgO-1-PO and AMS-MgO-1-PE sieved to 106 – 180 μm, respectively. As shown in Figures 4a, b, the CO_2 uptake capacity of AMS-MgO-1-PO increased rapidly in the initial five cycles, and then stabilized in the following 95 cycles, reaching a final CO_2 uptake of 0.53 $g_{CO2}/g_{sorbent}$ in the 100^{th} cycle. In contrast, the CO_2

uptake capacity of AMS-MgO-1-PE increased continuously over 100 cycles. AMS-MgO-1-PE exhibited an initial CO_2 uptake of 0.18 $g_{CO2}/g_{sorbent}$, ~ 50 % of that of the AMS-MgO-1-PO in the first cycle. The final CO_2 uptake capacity of AMS-MgO-1-PE after 100 cycles was 0.46 $g_{CO2}/g_{sorbent}$, which was close to that of AMS-MgO-1-PO (~ 0.53 $g_{CO2}/g_{sorbent}$). This was a surprising result since a reduction in the CO_2 uptake capacity after pelletization has been commonly reported for such sorbents, and that has been attributed to a significant deterioration in the pore structure (i.e., surface area and pore volume, as shown in Table 2).[3] Moreover, an irreversible mass increase (i.e., the observed baseline drift in Figure 4b) was present after the calcination stage (i.e., 400 °C, N_2) for AMS-MgO-1-PO and AMS-MgO-1-PE, which was related to the formation of the double salt $CaMg(CO_3)_2$ as confirmed by XRD (discussed below in Figure 6). The double salt $CaMg(CO_3)_2$ was very stable at the conditions employed here (carbonation: 350 °C, 80 vol.% CO_2; calcination: 400 °C, N_2), which is different from previous works[17,39,48] and may be related to the different synthesis method and molar ratios of (Li, K)NO_3 to (Na, K)$_2CO_3$ in the sorbents. From Figures 4c, d it can be seen that both AMS-MgO-1-PO and AMS-MgO-1-PE possessed fast CO_2 sorption rates, achieving more than 80 % of their final CO_2 uptake capacity within the first ten minutes. This is confirmed by performing an extended carbonation of 300 min at the 11th cycle shown in Figure S5 and Table S1, from which it is apparent that the additional increase in the CO_2 uptake after the initial ten minutes was small.

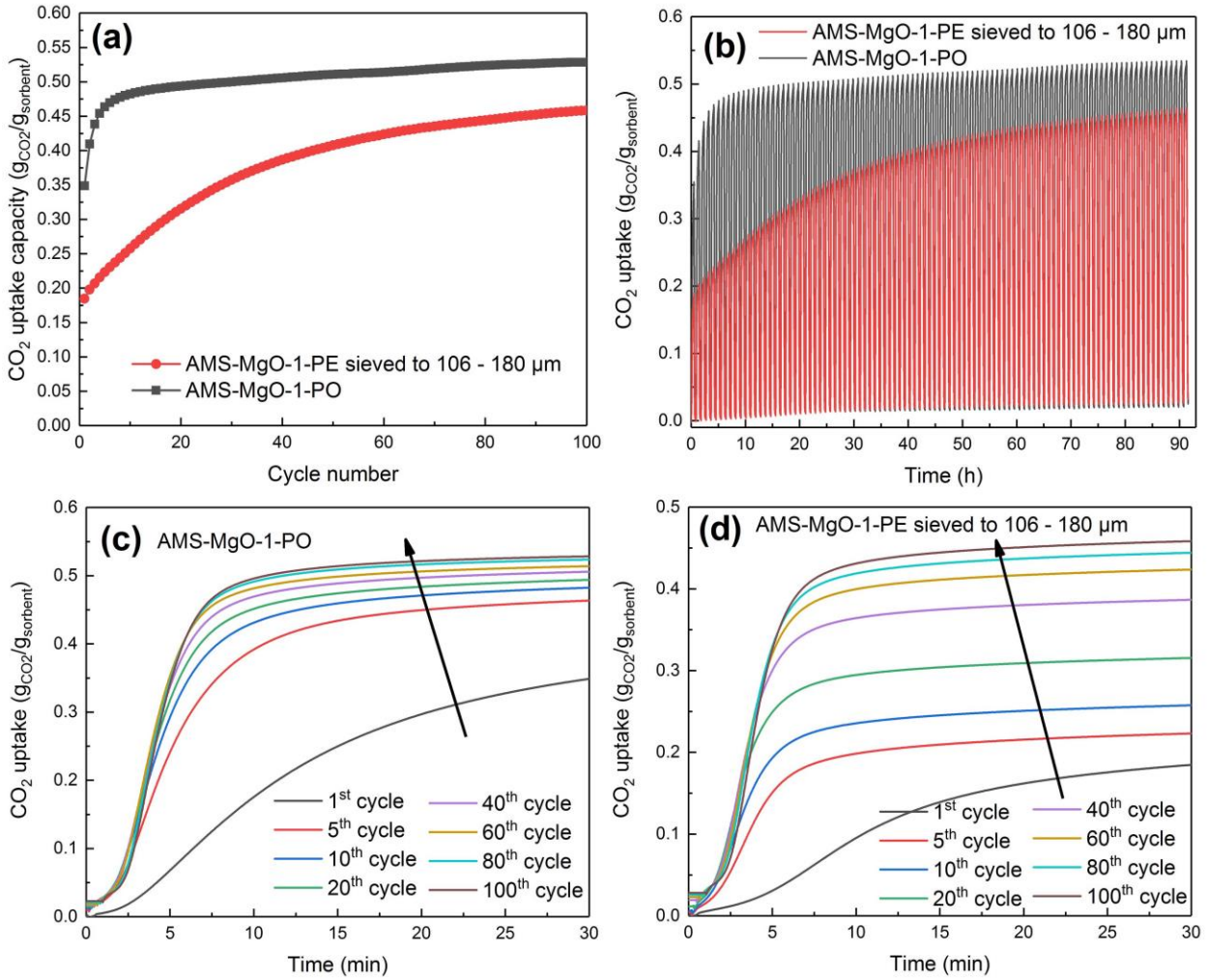

Figure 4. CO_2 capture performance of powdery and pelletized AMS-promoted MgO-based sorbents over 100 cycles in the TGA. (a) CO_2 uptake capacity as a function of cycle number, (b) CO_2 uptake as a function of reaction time, and CO_2 uptake of, respectively, (c) AMS-MgO-1-PO and (d) AMS-MgO-1-PE sieved to 106 – 180 μm as a function of reaction time for different cycles. The arrows in (c) and (d) indicate increasing cycle number. Reaction conditions: carbonation: 350 °C, 80 vol.% CO_2 (N_2 bal.), 30 min; calcination: 400 °C, N_2, 15 min.

To explain the continuous increase of the CO_2 uptake capacity for AMS-MgO-1-PE, a series of characterizations including ICP-OES, N_2 physisorption, SEM, and XRD, were conducted for

the as-synthesized and cycled samples. As is shown in Table 3, the relative mass ratios of the alkali metal ions (i.e., Li^+, K^+ and Na^+) to Mg^{2+} decreased during cyclic operation (Li^+:Mg^{2+} decreased from 0.014 to 0.012; K^+:Mg^{2+} decreased from 0.267 to 0.211; and Na^+:Mg^{2+} decreased from 0.105 to 0.088), which was most likely related to the evaporation of a small fraction of the alkali metal salts from the sorbent caused by the low melting temperature of this particular mixture (~ 300 °C as shown in Figure S6). However, the relative mass ratio between Li^+, K^+, and Na^+ was still relatively constant, implying that the stoichiometry of the mixture was not affected during the cycling experiment and there was not a preferential loss of particular alkali species. Observing an increase in the CO_2 uptake despite a decreasing amount of AMS in the sorbent was unexpected. The AMS itself possessed a low cyclic CO_2 uptake capacity (~ 7.6×10^{-4} $g_{CO2}/g_{material}$), as can be seen from the small mass increase during the carbonation reaction when 20 wt.% AMS was loaded onto a SiO_2 support (as shown in Figure S7).

Table 3. N_2 physisorption and ICP-OES results of the as-synthesized and cycled AMS-MgO-1-PE sieved to 106 – 180 μm after the TGA experiments.

Sample	N_2 physisorption results		Relative mass ratio[a]				
	Surface area (m^2/g)	Pore volume (cm^3/g)	Ca : Mg	Li : Mg	K : Mg	Na : Mg	Li : K : Na
As-synthesized	7.3	0.051	0.152	0.014	0.267	0.105	3.7 : 69.1 : 27.2
After 1st calcination	2.9	0.009	0.151	0.012	0.226	0.089	3.8 : 69.0 : 27.2
After 1 cycle[c]	4.9	0.013	0.149	0.013	0.231	0.090	3.8 : 69.2: 27.0
After 5 cycles[c]	2.8	0.011	0.150	0.012	0.230	0.090	3.7 : 69.1 : 27.2
After 10 cycles[c]	3.3	0.010	0.149	0.012	0.224	0.089	3.7 : 69.0 : 27.3
After 20 cycles[c]	3.6	0.010	0.150	0.012	0.224	0.090	3.8 : 68.6 : 27.7
After 30 cycles[c]	0.8	0.007	0.149	0.012	0.221	0.089	3.7 : 68.6 : 27.7
After 50 cycles[c]	0.7	0.008	0.149	0.012	0.215	0.088	3.8 : 68.4 : 27.9
After 100 cycles[c]	N/A[b]	N/A	0.149	0.012	0.211	0.088	3.7 : 68.0 : 28.3

a: Obtained by ICP-OES.
b: Not available.
c: Collected after the calcination stage

Turning to the N_2 physisorption results of the as-synthesized and cycled sorbents (Table 3), it was found that the surface area and pore volume decreased significantly after the first calcination.

After one carbonation/calcination cycle, both surface area and pore volume increased slightly and were then relatively stable in the subsequent 19 cycles. With increasing cycle number, a further considerable reduction in the surface area and pore volume of the sorbents took place. Similar results were also obtained for the sorbents that underwent eight cycles in a packed bed reactor (discussed below, Table S2). Analyzing the pore size distributions of the cycled sorbents in detail, we observed the disappearance of pore volume in the mesoporous range and an increase in pore volume in the range of micropores during cyclic operation (Figure 5a). Figures 5b-f show the evolution of the surface morphology of the as-synthesized and cycled sorbents through SEM. The surface of the sorbents was relatively coarse during cycling, and only slight sintering of the MgO was observed when the sorbents had undergone up to 50 cycles (Figures 5b-e). Particle agglomeration was observed only for the sorbents that have undergone 100 cycles (Figure 5f). However, the crystallite size of the MgO estimated by the Scherrer equation was very stable during cyclic operation and increased only marginally from 34 to 41 nm (as shown in Figure S8). Therefore, considering the continuously increasing CO_2 uptake during cyclic operation shown in Figure 4, the morphological changes of the sorbents do not seem to have played an important role in this trend. Yet, the morphological changes may have enhanced the CO_2 capture performance in the initial cycles to some extent, due to the increased surface area and pore volume as shown in Table 3.

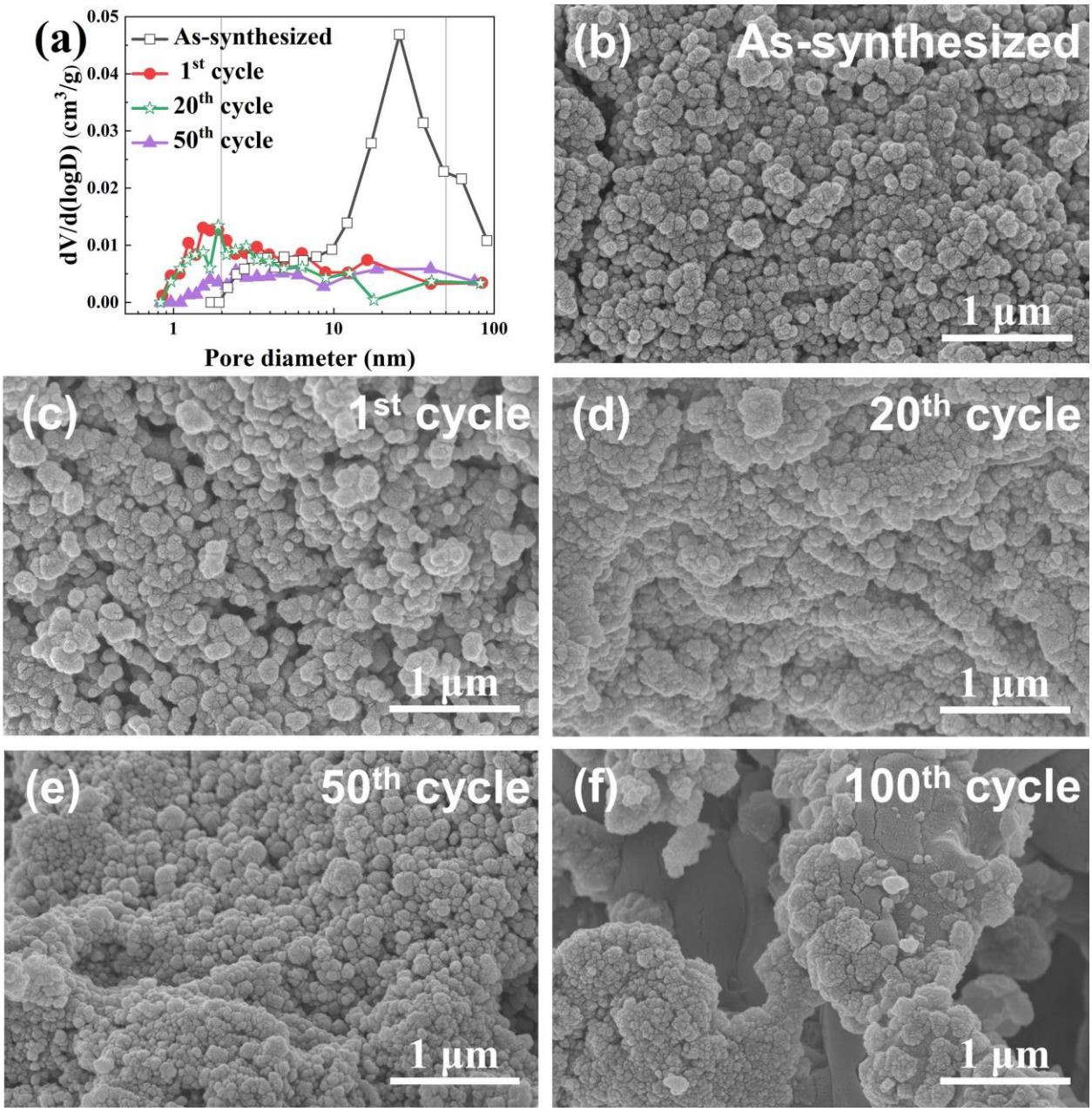

Figure 5. Evolution of the pore size distribution and morphologies of AMS-MgO-1-PE sieved to 106 – 180 µm over 100 cycles in the TGA. (a) Pore size distribution, and SEM images of (b) as-synthesized sorbent and sorbents after (c) one cycle, (d) 20 cycles, (e) 50 cycles and (f) 100 cycles. Reaction conditions: carbonation: 350 °C, 80 vol.% CO_2 (N_2 bal.), 30 min; calcination: 400 °C,

N_2, 15 min. The vertical grey lines indicate the microporous (< 2 nm) and mesoporous (2 – 50 nm) ranges, respectively. The samples were collected after the calcination stage.

XRD characterization was conducted for powdery and pelletized, AMS-promoted, MgO-based sorbents that underwent different numbers of cycles (measured after the calcination reaction). We note that the characterization was carried out at room temperature when all phases existed in a solid state, whereas the AMS nitrates are typically molten at the carbonation and calcination temperatures employed in this work. As shown in Figure 6 and Figure S9, the powdery and pelletized sorbents possessed the same principal chemical compositions after cyclic operation (collected after the calcination stage), including MgO, KNO_3, $CaMg(CO_3)_2$, Na_2CO_3, $CaCO_3$, and K_2CO_3. However, it is surprising to observe that there was hardly any phase transformation in the powdery sorbents compared to the pelletized sorbents. Three different KNO_3 phases (i.e., 00-015-0607, 01-071-1558, and 01-078-7937) were present in the pelletized sorbents, whereas only one KNO_3 phase (i.e., 01-078-7937) was present in the powdery sorbents; we note that the nitrate phase may have undergone polymorphic changes during the cooling to room temperature.[51] Details of the crystallographic parameters of these KNO_3 phases can be found in Table S3. Consequently, we speculate that the nature of the alkali species (mostly the nitrates) within the molten phase has changed during cycling; this led to a different re-crystallization behavior upon cooling that followed a systematic trend with cycling as observed by XRD at ambient temperature. It would appear that with the transformation of the AMS species their physical properties changed (e.g., the solubility of carbonate and oxide ions and CO_2), which lead to a continuous increase in the CO_2 uptake with cycling. Interestingly, the CO_2 uptake of the powdery and pelletized sorbents was very similar after 100 cycles (Figure 4a), despite the presence of different KNO_3 phases that imply the nature of the molten phase was different in these two sorbents.

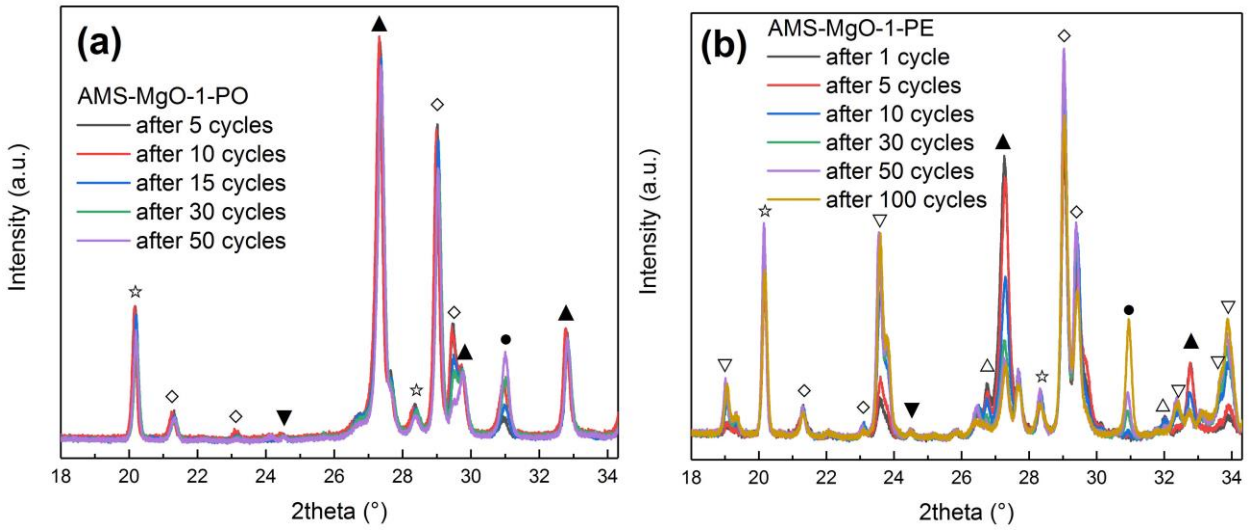

Figure 6. Crystalline phases of powdery and pelletized AMS-promoted MgO-based sorbents for different cycle numbers. XRD patterns of (a) AMS-MgO-1-PO and (b) AMS-MgO-1-PE sieved to 106 – 180 μm after different cycles in the TGA (collected after the calcination stage). △: KNO_3, 00-015-0607; ▽: KNO_3, 01-071-1558; ▲: KNO_3, 01-078-7937; ●: $CaMg(CO_3)_2$, 00-036-0426; ◇: $CaCO_3$, 01-072-1214; ☆: K_2CO_3, 07-073-5067; ▼: Na_2CO_3, 01-086-0299.

Effect of the CO_2 concentration in the carbonation/calcination stages

It has been widely reported that the CO_2 concentration present in the carbonation and calcination stages, respectively, plays a crucial role in the CO_2 capture performance of the sorbents.[52] As is shown in Figures 7a, b, the CO_2 concentration in the carbonation stage affected both the observed CO_2 sorption rate and the CO_2 uptake capacity significantly. When the CO_2 concentration was below 15 vol.%, the CO_2 uptake was negligible, reaching a maximum of 0.004 $g_{CO2}/g_{sorbent}$ after carbonation for 30 min. With an increase in the CO_2 concentration from 15 to 40 vol.%, the CO_2 uptake capacity increased but was still less than 0.04 $g_{CO2}/g_{sorbent}$. Only when the CO_2 concentration was greater than 50 vol.% was a significant increase in the CO_2 uptake

observed. In particular, there was only a marginal further increase in the CO_2 uptake capacity when the CO_2 concentration was greater than 60 vol.%.

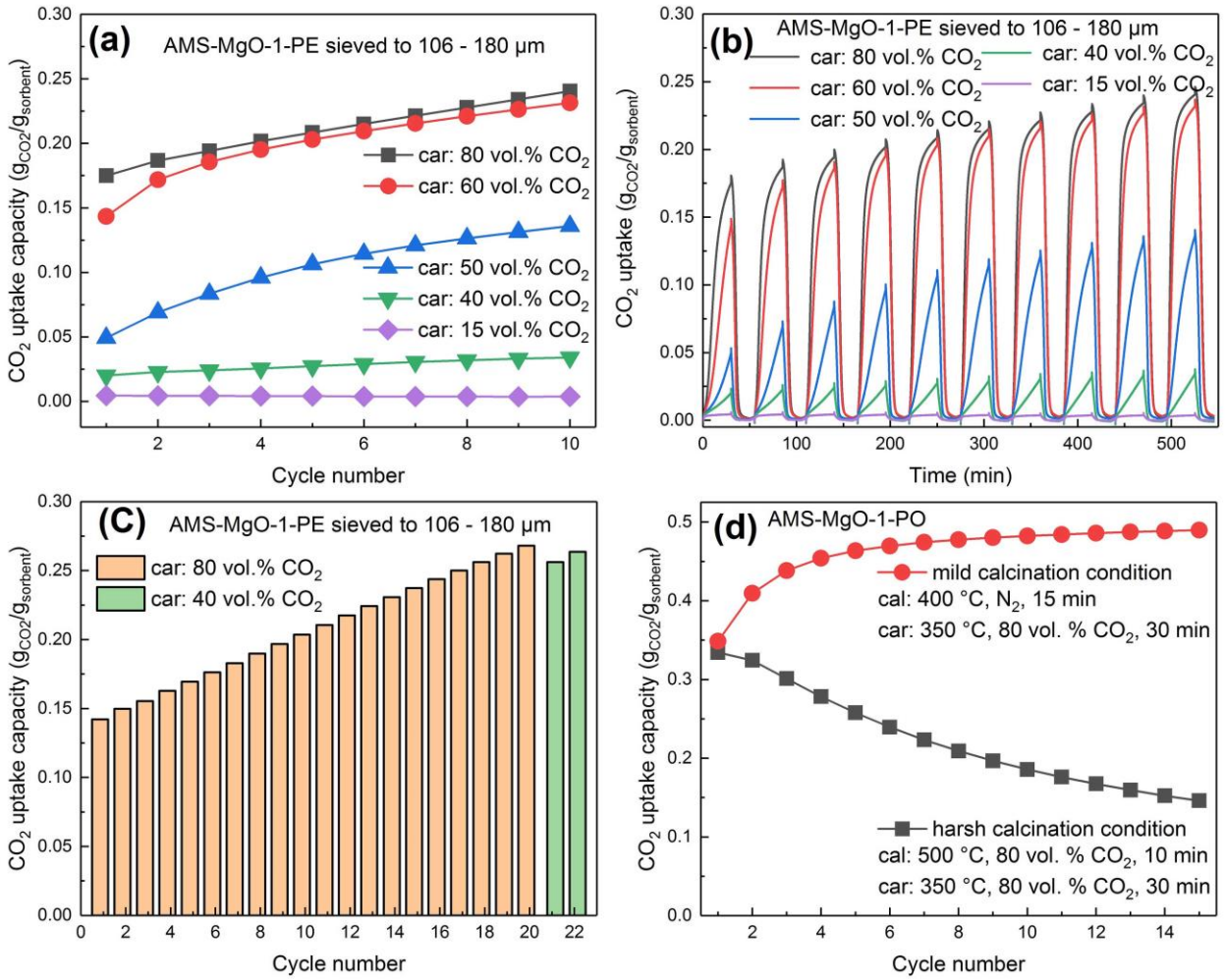

Figure 7. CO_2 capture performance of AMS-promoted MgO-based sorbents (AMS-MgO-1-PE or AMS-MgO-1-PO) in different CO_2 concentrations in the calcination or carbonation stage in the TGA (collected after the calcination stage). (a) CO_2 uptake capacity as a function of cycle number in different CO_2 concentrations in the carbonation stage, (b) CO_2 uptake as a function of reaction time in different CO_2 concentrations in the carbonation stage, (c) CO_2 uptake capacity as a function of cycle number in decreased CO_2 concentrations in the last two carbonation cycles, and (d) CO_2

uptake capacity as a function of cycle number under different CO_2 concentrations in the calcination stage. Reaction conditions in (a-c): carbonation: 350 °C, 30 min; calcination: 400 °C, N_2, 30 min.

XRD characterization was conducted for the pelletized AMS-promoted MgO-based sorbents in different carbonation atmospheres (i.e., 15 vol.% and 80 vol.% CO_2) after ten cycles. As is shown in Figure S10, most significantly the KNO_3 phase (i.e., 01-071-1558) was absent when the cyclic experiment was conducted in a lower CO_2 concentration in the carbonation stage. Thus, it seems that a high CO_2 concentration in the carbonation step was required to enable the transformation of the AMS species in the molten phase (which resulted in different crystalline alkali phases within the material upon cooling down to room temperature), thus inducing an increase in the reactivity of the AMS-promoted MgO-based sorbents. This was further confirmed by an additional experiment shown in Figure 7c: AMS-MgO-1-PE exhibited an increasing CO_2 uptake capacity in the initial 20 cycles (i.e., from 0.14 to 0.27 $g_{CO2}/g_{sorbent}$) when 80 vol.% CO_2 was used in the carbonation reaction. The CO_2 concentration was then reduced from 80 vol.% to 40 vol.% in the subsequent two cycles. Although the CO_2 concentration was reduced by 50 %, a negligible reduction in the CO_2 uptake capacity (~ 4.4 %) was observed. The sorbent achieved a CO_2 uptake capacity of 0.26 $g_{CO2}/g_{sorbent}$ when the CO_2 concentration was reduced from 80 vol.% to 40 vol.%, which was much higher compared to when the sorbent was cycled in a consistent CO_2 concentration of 40 vol.% during the carbonation stage (Figure 7a). It thus would appear that the high CO_2 concentration present during carbonation activated the sorbent somehow, such that CO_2 sorption was feasible also under lower CO_2 concentrations (but still not in 15 vol.% CO_2 as shown in Figure S11). We speculate that the transformation of the AMS species observed in Figure 6b altered their physical properties in the molten phase (e.g., the melting temperature as shown in Figure S6, or the solubility of CO_2 and possibly of MgO and the carbonates) such that fast CO_2

sorption is feasible also under conditions that in the absence of an AMS promoter (or in the presence of the as-synthesized AMS) would be thermodynamically unfavorable. It is noted that further investigations are required to understand better what physical properties of the AMS mixture are required to enable the fast sorption of CO_2 on MgO and how the AMS, MgO and CO_2 interact on a molecular level.

In order to obtain a highly concentrated CO_2 stream at the outlet of the calcination reactor, a high CO_2 concentration is typically used in the calcination reactor. Thus, the effect of the CO_2 concentration in the calcination reaction was also investigated. Note that for thermodynamic reasons, a higher calcination temperature is required when a high CO_2 concentration is used in the calcination stage (Figure S12). However, as is shown in Figure 7d, the CO_2 uptake capacity of the sorbents decreased substantially when the calcination reaction took place under a high CO_2 concentration (i.e., 80 vol.% CO_2, as may be required in an industrially-relevant process). To explain the significant decline in the CO_2 capture performance, XRD and SEM characterizations were conducted for the sorbents after exposure to N_2 or CO_2, which is given in Figures S13a-d. It can be found that the MgO crystallite size estimated by the Scherrer equation increased from ~ 34 to ~ 40 nm after exposure to CO_2 during the calcination reaction, whereas it was only ~ 34 nm after exposure to N_2. Moreover, significant agglomeration was observed only for the sorbent after exposure to CO_2. Both the increase in MgO crystallite size and the agglomeration resulted in an obvious decline in the subsequent CO_2 uptake capacity, as shown in Figures S13e, f, although the sorbent underwent only one carbonation/calcination cycle. Therefore, the rapid decline in the CO_2 uptake capacity when a high CO_2 concentration was used in the calcination stage was caused by the severe sintering of the $MgCO_3$ upon decomposition.

<u>CO_2 capture performance in a packed bed reactor</u>

The CO_2 capture performance of the best-performing powdery and pelletized sorbents, i.e., AMS-MgO-1-PO and AMS-MgO-1-PE sieved to 106 – 180 μm, was evaluated in a packed bed reactor with a long gas-solid contact time (i.e., 10000 mL/($g_{sorbent}$·h)), to assess whether the most reactive sorbents are capable of removing a significant amount of CO_2 from a gas stream under such conditions. Figure S14 shows the CO_2 capture performance of AMS-promoted MgO-based sorbents measured at carbonation temperature of 300 °C over ten cycles in the TGA, which demonstrates an obvious decline in the CO_2 uptake capacity after initial several cycles rather than the continuous increase as observed in Figure 4; we speculate that the carbonation temperature was too low for a substantial fraction of the AMS to be molten, and this fraction decreased with cycling as alkali phases transformed. Therefore, only 325 or 350 °C was used as the carbonation temperature in the packed bed experiments. The measured CO_2 concentration of eight cycles plotted as a function of reaction time using AMS-MgO-1-PO and AMS-MgO-1-PE sieved to 106 – 180 μm is given in Figure S15, and the corresponding CO_2 uptake capacity as a function of cycle number is shown in Figure 8a. Similar to the TGA experiments, the CO_2 uptake capacity of AMS-MgO-1-PE sieved to 106 – 180 μm increased with cycling from 0.12 to 0.17 $g_{CO2}/g_{sorbent}$ in the eighth cycle. AMS-MgO-1-PO had a relatively stable CO_2 capture performance after the initial cycles. The results from the packed bed experiments thus agreed well with that from the TGA experiments (i.e., Figure 4 and Figure S4) and showed that the sorbents can relatively quickly be converted from MgO to $MgCO_3$.

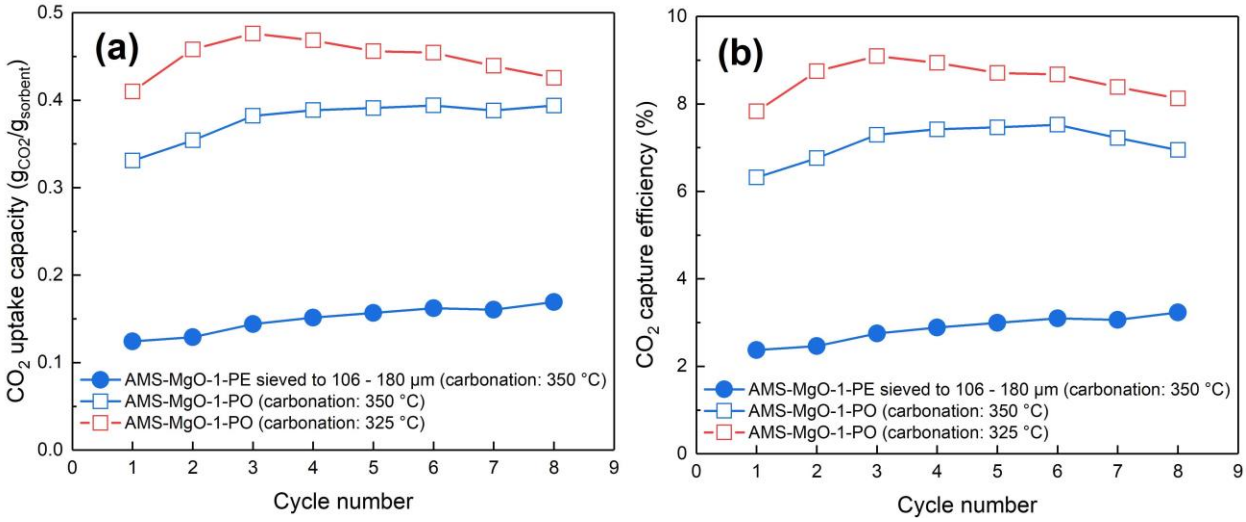

Figure 8. CO_2 capture performance of powdery and pelletized AMS-promoted MgO-based sorbents over eight cycles at different conditions in the packed bed reactor. (a) CO_2 uptake capacity as a function of cycle number, and (b) CO_2 capture efficiency as a function of cycle number. Reaction conditions: carbonation: 325 or 350 °C, 80 vol.% CO_2 (N_2 bal.), 30 min; calcination: 400 °C, N_2, 30 min.

Herein the AMS-promoted MgO-based sorbents demonstrated comparatively high CO_2 uptake capacities in both the TGA and the packed bed reactor (as compared in Table 1); however, the CO_2 capture efficiency of such sorbents under the specific conditions tested here was low (less than 10 %, as shown in Figure 8b), implying that most of the CO_2 entering the reactor was not captured by the sorbent. From an industrial application point of view, the CO_2 capture efficiencies at the specific contact times assessed here are probably too low for a CO_2 capture process to be economically feasible (which, however, needs to be assessed in a separate work), raising also doubts whether the MgO/$MgCO_3$-system is even conceptually suitable for CO_2 capture at ambient pressure (note that the carbonation was performed in 80 vol.% CO_2, i.e., much higher than what any industrial process would emit into the atmosphere). Hu et al.[38] have demonstrated that AMS-

promoted MgO can indeed remove most of the CO_2 from a gas stream, but this required partial pressures of CO_2 greater than several bars and is thus more suitable for pre-combustion CO_2 capture processes (e.g., the sorption-enhanced water gas shift reaction). Their results also imply that the formation of $MgCO_3$ is not only kinetically problematic, but also thermodynamically. Most previous studies on CO_2 capture using MgO focused on improving the observed rate of formation of $MgCO_3$, but neglected that the reaction conditions for achieving high sorption rates are unfavorable for achieving high CO_2 capture efficiencies. As shown in this work, such material developments have limited potential in post-combustion CO_2 capture due to the low CO_2 concentrations involved (10 – 20 vol.%) at ambient pressure, but they may be promising as sorbents in pre-combustion CO_2 capture because of the higher CO_2 concentrations (30 – 60 vol.%) at a total pressure typically greater than 10 bar.[53] Importantly, new effective sorbents need to be optimized such that the AMS exist in molten state to enable fast CO_2 sorption rates at low temperatures (ideally < 300 °C) for which thermodynamic limitations are reduced and theoretically high CO_2 capture efficiencies can be achieved also for low CO_2 concentrations.

CONCLUSION

The most reactive MgO-based sorbents that have been reported in the literature, i.e., MgO promoted with a combination of various AMS (incl. $NaNO_3$, $LiNO_3$, K_2CO_3 and Na_2CO_3) were investigated in this work, including an assessment of the effect of particle size (from powder to pelletized 500 μm particles) and reaction conditions (calcination/carbonation temperature, and partial pressure of CO_2) on the cyclic CO_2 capture performance using a TGA at ambient pressure. The TGA results showed that the CO_2 uptake capacity of the sorbents decreased significantly after pelletization, losing 74 % of their initial capacity. The pelletized sorbents had similar CO_2 uptake capacities when varying the particle size. However, it is surprising that the CO_2 uptake capacity of

pelletized sorbents increased constantly over 100 cycles, which was 0.46 $g_{CO2}/g_{sorbent}$ at the 100th cycle and hence very close to that of the powdery sample (~ 0.53 $g_{CO2}/g_{sorbent}$). It is speculated that the increase was related to a change of the nature of the alkali species in the molten phase during cycling. Such a transformation took place when only a high CO_2 partial pressure (greater than 0.6 bar) was used in the carbonation reaction, then enabling a relatively good CO_2 capture performance even when the CO_2 partial pressure was reduced to 0.4 bar. In addition, the CO_2 capture performance of the best-performing sorbents was evaluated in a packed bed reactor to assess whether the most reactive, state-of-the-art MgO-based sorbents are actually capable of removing a significant amount of CO_2 from a gas stream. The CO_2 uptake of the sorbents in the packed bed experiments was very close to that in the TGA experiments, but the CO_2 capture efficiency was less than 10 %, under the conditions studied here, and thus probably too low for an industrial process. Current state-of-the-art AMS-promoted MgO-based sorbents appear to have limited potential in post-combustion CO_2 capture, but they may be promising as sorbents in pre-combustion CO_2 capture because of the higher CO_2 partial pressures involved (typically > 5 bar). For the development of new AMS-promoted MgO-based sorbents that are potentially suitable for post-combustion CO_2 capture, the transformation of the alkali phases needs to be considered, which may depend on both temperature and CO_2 concentration. More work is required to understand how the CO_2 sorption properties of AMS-promoted MgO-based sorbents are related to the physical and chemical properties of the alkali mixture under different reaction conditions.

ASSOCIATED CONTENT

Supporting Information.

This information is available free of charge via the Internet at http://pubs.acs.org.

CO_2 capture performance of AMS-MgO-1-PO and AMS-MgO-1-PO-Ref in the TGA; Long cyclic performance of AMS-MgO-2-PE sieved to 106 – 180 μm at optimal carbonation/calcination temperatures in the TGA; CO_2 capture performance of AMS-MgO-1-PE and AMS-MgO-0.5-PE sieved to 106 – 180 μm at different carbonation and calcination temperatures in the TGA; CO_2 capture performance of AMS-MgO-1-PO at different carbonation temperatures in the TGA; CO_2 capture performance of AMS-MgO-1-PO under an extended carbonation duration in the 11^{th} cycle in the TGA; DSC profiles of 60 wt.% AMS/SiO_2 and AMS-MgO-1-PE sieved to 106 -180 μm after different cycles in the TGA; CO_2 capture performance of AMS/SiO_2 over five cycles in the TGA; Surface area and pore volume of the as-synthesized and cycled AMS-MgO-1-PO and AMS-MgO-1-PE sieved to 106 – 180 μm after the packed bed experiments; Evolution of the MgO crystallite sizes in AMS-MgO-1-PE sieved to 106 – 180 μm during cyclic operation in the TGA; Crystalline phases of AMS-MgO-1-PO and AMS-MgO-1-PE sieved to 106 – 180 μm after 50 and 100 cycles in the TGA, respectively; Crystallographic parameters of the KNO_3 phases present in the powdery and pelletized AMS-promoted MgO-based sorbents during cycling in the TGA; Crystalline phases of pelletized AMS-promoted MgO-based sorbents under different carbonation atmospheres after ten cycles in the TGA; CO_2 uptake capacity of AMS-MgO-1-PE sieved to 106 – 180 μm as a function of cycle number in the TGA under decreased CO_2 concentrations in the last two carbonation cycles; Decomposition characteristics of the carbonated AMS-MgO-1-PO under different heating atmospheres measured in the TGA; Changes of MgO crystallite sizes, morphology and CO_2 capture performance after exposure to CO_2 or N_2 for AMS-MgO-1-PO; CO_2 uptake capacity of AMS-MgO-1-PO and AMS-MgO-1-PE sieved to 106 – 180 μm as a function of cycle number at carbonation temperature of 300 °C in the TGA; Measured CO_2 concentration

of eight cycles plotted as a function of reaction time using pelletized and powdery AMS-promoted MgO-based sorbents at different conditions in the packed bed reactor; CO_2 capture performance of AMS-MgO-1-PO at different carbonation temperatures in the TGA.

AUTHOR INFORMATION

Corresponding Author

*Email: duanlunbo@seu.edu.cn; donatf@ethz.ch; muelchri@ethz.ch

Author Contributions

J.C. prepared the sorbents and did the experimental work except the ICP-OES and SEM work. J.C. and F.D. analyzed and discussed the experimental results. F.D. performed the ICP-OES analysis. J.C. wrote the manuscript, and F.D., L.D. and C.M. revised the manuscript. All authors have given approval to the final version of the manuscript.

Funding Sources

The authors wish to acknowledge the financial support from the National Natural Science Foundation of China (51922027), the Scientific Research Foundation of Graduate School of Southeast University, China (YBPY1902), the Program of China Scholarships Council (No. 201806090031), the Fundamental Research Funds for the Central Universities, the Swiss National Science Foundation (156015), and the European Research Council (ERC) under the European Union's Horizon 2020 research and innovation programme under grant agreement No. 819573.

Notes

The authors declare no competing financial interest.

ACKNOWLEDGMENT

We acknowledge the financial support from the National Natural Science Foundation of China (51922027), the Scientific Research Foundation of Graduate School of Southeast University, China (YBPY1902), the Program of China Scholarships Council (No. 201806090031), the Fundamental Research Funds for the Central Universities, and the Swiss National Science Foundation (156015). C.M. acknowledges funding from the European Research Council (ERC) under the European Union's Horizon 2020 research and innovation program grant agreement No. 819573. We also thank Maximilian Krödel and Lorenz Abduly for discussion, Agnieszka Kierzkowska for performing SEM characterization, and the Scientific Center for Optical and Electron Microscopy (ScopeM) of ETH Zurich for providing access to SEM facilities.

REFERENCES

(1) Kierzkowska, A. M.; Pacciani, R.; Müller, C. R. CaO-Based CO_2 Sorbents: From Fundamentals to the Development of New, Highly Effective Materials. *ChemSusChem* **2013**, *6* (7), 1130–1148.

(2) Yan, Y.; Wang, K.; Clough, P. T.; Anthony, E. J. Developments in Calcium/Chemical Looping and Metal Oxide Redox Cycles for High-Temperature Thermochemical Energy Storage: A Review. *Fuel Process. Technol.* **2020**, *199* (November 2019), 106280.

(3) Chen, J.; Duan, L.; Sun, Z. Review on the Development of Sorbents for Calcium Looping. *Energy & Fuels* **2020**, *34* (7), 7806–7836.

(4) Wang, J.; Huang, L.; Yang, R.; Zhang, Z.; Wu, J.; Gao, Y.; Wang, Q.; O'Hare, D.; Zhong, Z. Recent Advances in Solid Sorbents for CO_2 Capture and New Development Trends. *Energy Environ. Sci.* **2014**, *7* (11), 3478–3518.

(5) Gao, W.; Zhou, T.; Gao, Y.; Louis, B.; O'Hare, D.; Wang, Q. Molten Salts-Modified MgO-Based Adsorbents for Intermediate-Temperature CO_2 Capture: A Review. *J. Energy Chem.*

2017, *26* (5), 830–838.

(6) Chen, J.; Duan, L.; Donat, F.; Müller, C. R.; Anthony, E. J.; Fan, M. Self-Activated, Nanostructured Composite for Improved CaL-CLC Technology. *Chem. Eng. J.* **2018**, *351* (June), 1038–1046.

(7) Chen, J.; Duan, L.; Shi, T.; Bian, R.; Lu, Y.; Donat, F.; Anthony, E. J. A Facile One-Pot Synthesis of CaO/CuO Hollow Microspheres Featuring Highly Porous Shells for Enhanced CO_2 Capture in a Combined Ca–Cu Looping Process via a Template-Free Synthesis Approach. *J. Mater. Chem. A* **2019**, *7* (37), 21096–21105.

(8) Chen, J.; Donat, F.; Duan, L.; Kierzkowska, A. M.; Kim, S. M.; Xu, Y.; Anthony, E. J.; Müller, C. R. Metal-Oxide Stabilized CaO/CuO Composites for the Integrated Ca/Cu Looping Process. *Chem. Eng. J.* **2021**, *403* (May 2020), 126330.

(9) Yang, X.; Zhao, L.; Liu, Y.; Sun, Z.; Xiao, Y. Carbonation Performance of $NaNO_3$ Modified MgO Sorbents. *Ind. Eng. Chem. Res.* **2017**, *56* (1), 342–350.

(10) Hwang, B. W.; Lim, J. H.; Chae, H. J.; Ryu, H.-J.; Lee, D.; Lee, J. B.; Kim, H.; Lee, S. C.; Kim, J. C. CO_2 Capture and Regeneration Properties of MgO-Based Sorbents Promoted with Alkali Metal Nitrates at High Pressure for the Sorption Enhanced Water Gas Shift Process. *Process Saf. Environ. Prot.* **2018**, *116*, 219–227.

(11) Zarghami, S.; Hassanzadeh, A.; Arastoopour, H.; Abbasian, J. Effect of Steam on the Reactivity of MgO-Based Sorbents in Precombustion CO_2 Capture Processes. *Ind. Eng. Chem. Res.* **2015**, *54* (36), 8860–8866.

(12) Guo, Y.; Tan, C.; Sun, J.; Li, W.; Zhao, C.; Zhang, J.; Lu, P. Nanostructured MgO Sorbents Derived from Organometallic Magnesium Precursors for Post-Combustion CO_2 Capture. *Energy & Fuels* **2018**, *32* (6), 6910–6917.

(13) Yang, L.; Liu, D.; Wang, P.; Seo, H.; Gui, J.; Park, Y.-K. Toward the Insights into Fast CO_2 Absorption over Novel Nanostructured MgO-Based Sorbent. *Ind. Eng. Chem. Res.* **2018**, *57* (31), 10591–10600.

(14) Hanif, A.; Dasgupta, S.; Nanoti, A. Facile Synthesis of High-Surface-Area Mesoporous MgO with Excellent High-Temperature CO_2 Adsorption Potential. **2016**.

(15) Han, S. J.; Bang, Y.; Kwon, H. J.; Lee, H. C.; Hiremath, V.; Song, I. K.; Seo, J. G. Elevated Temperature CO_2 Capture on Nano-Structured MgO–Al_2O_3 Aerogel: Effect of Mg/Al Molar Ratio. *Chem. Eng. J.* **2014**, *242*, 357–363.

(16) Hiremath, V.; Shavi, R.; Seo, J. G. Controlled Oxidation State of Ti in MgO-TiO_2 Composite for CO_2 Capture. *Chem. Eng. J.* **2017**, *308*, 177–183.

(17) Liu, S.; Zhang, X.; Li, J.; Zhao, N.; Wei, W.; Sun, Y. Preparation and Application of Stabilized Mesoporous MgO-ZrO_2 Solid Base. *Catal. Commun.* **2008**, *9* (7), 1527–1532.

(18) Cui, H.; Cheng, Z.; Zhou, Z. Unravelling the Role of Alkaline Earth Metal Carbonates in Intermediate Temperature CO_2 capture Using Alkali Metal Salt-Promoted MgO-Based Sorbents. *J. Mater. Chem. A* **2020**, *8* (35), 18280–18291.

(19) Lee, C. H.; Mun, S.; Lee, K. B. Characteristics of Na-Mg Double Salt for High-Temperature CO_2 Sorption. *Chem. Eng. J.* **2014**, *258*, 367–373.

(20) Zhang, K.; Li, X. S.; Li, W. Z.; Rohatgi, A.; Duan, Y.; Singh, P.; Li, L.; King, D. L. Phase Transfer-Catalyzed Fast CO_2 Absorption by MgO-Based Absorbents with High Cycling Capacity. *Adv. Mater. Interfaces* **2014**, *1* (3), 1–6.

(21) Dunstan, M. T.; Donat, F.; Bork, A. H.; Grey, C. P.; Müller, C. R. CO_2 Capture Using Solid Sorbents: Fundamental Aspects, Mechanistic Insights and Recent Advances. https://engrxiv.org/y654z/

(22) Park, S. J.; Kim, Y.; Jones, C. W. $NaNO_3$-Promoted Mesoporous MgO for High-Capacity CO_2 Capture from Simulated Flue Gas with Isothermal Regeneration. *ChemSusChem* **2020**, *13* (8), 2988–2995.

(23) Triviño, M. L. T.; Hiremath, V.; Seo, J. G. Stabilization of $NaNO_3$-Promoted Magnesium Oxide for High-Temperature CO_2 Capture. *Environ. Sci. Technol.* **2018**, *52* (20), 11952–11959.

(24) Jo, S. I.; An, Y. I.; Kim, K. Y.; Choi, S. Y.; Kwak, J. S.; Oh, K. R.; Kwon, Y. U. Mechanisms of Absorption and Desorption of CO_2 by Molten $NaNO_3$-Promoted MgO. *Phys. Chem. Chem. Phys.* **2017**, *19* (8), 6224–6232.

(25) Gao, W.; Zhou, T.; Gao, Y.; Wang, Q.; Lin, W. Study on MNO_3/NO_2 (M = Li, Na, and K)/MgO Composites for Intermediate-Temperature CO_2 Capture. *Energy & Fuels* **2019**, *33* (3), 1704–1712.

(26) Wang, K.; Zhao, Y.; Clough, P. T.; Zhao, P.; Anthony, E. J. Structural and Kinetic Analysis of CO_2 Sorption on $NaNO_2$-Promoted MgO at Moderate Temperatures. *Chem. Eng. J.* **2019**, *372* (April), 886–895.

(27) Vu, A.-T.; Park, Y.; Jeon, P. R.; Lee, C.-H. Mesoporous MgO Sorbent Promoted with KNO_3 for CO_2 Capture at Intermediate Temperatures. *Chem. Eng. J.* **2014**, *258*, 254–264.

(28) Lee, H.; Trivinìo, M. L. T.; Hwang, S.; Kwon, S. H.; Lee, S. G.; Moon, J. H.; Yoo, J.; Seo, J. G. In Situ Observation of Carbon Dioxide Capture on Pseudo-Liquid Eutectic Mixture-Promoted Magnesium Oxide. *ACS Appl. Mater. Interfaces* **2018**, *10* (3), 2414–2422.

(29) Vu, A. T.; Ho, K.; Jin, S.; Lee, C. H. Double Sodium Salt-Promoted Mesoporous MgO Sorbent with High CO_2 Sorption Capacity at Intermediate Temperatures under Dry and Wet Conditions. *Chem. Eng. J.* **2016**, *291*, 161–173.

(30) Zhao, X.; Ji, G.; Liu, W.; He, X.; Anthony, E. J.; Zhao, M. Mesoporous MgO Promoted with $NaNO_3/NaNO_2$ for Rapid and High-Capacity CO_2 Capture at Moderate Temperatures. *Chem. Eng. J.* **2018**, *332* (July 2017), 216–226.

(31) Zhang, K.; Li, X. S.; Chen, H.; Singh, P.; King, D. L. Molten Salt Promoting Effect in Double Salt CO_2 Absorbents. *J. Phys. Chem. C* **2016**, *120* (2), 1089–1096.

(32) Dal Pozzo, A.; Armutlulu, A.; Rekhtina, M.; Abdala, P. M.; Müller, C. R. CO_2 Uptake and Cyclic Stability of MgO-Based CO_2 Sorbents Promoted with Alkali Metal Nitrates and Their Eutectic Mixtures. *ACS Appl. Energy Mater.* **2019**, *2* (2), 1295–1307.

(33) Qiao, Y.; Wang, J.; Zhang, Y.; Gao, W.; Harada, T.; Huang, L.; Hatton, T. A.; Wang, Q. Alkali Nitrates Molten Salt Modified Commercial MgO for Intermediate-Temperature CO_2 Capture: Optimization of the Li/Na/K Ratio. *Ind. Eng. Chem. Res.* **2017**, *56* (6), 1509–1517.

(34) Wang, J.; Li, M.; Lu, P.; Ning, P.; Wang, Q. Kinetic Study of CO_2 Capture on Ternary Nitrates Modified MgO with Different Precursor and Morphology. *Chem. Eng. J.* **2020**, *392* (December 2019), 123752.

(35) Harada, T.; Simeon, F.; Hamad, E. Z.; Hatton, T. A. Alkali Metal Nitrate-Promoted High-Capacity MgO Adsorbents for Regenerable CO_2 Capture at Moderate Temperatures. *Chem. Mater.* **2015**, *27* (6), 1943–1949.

(36) Jin, S.; Ho, K.; Lee, C.-H. Facile Synthesis of Hierarchically Porous MgO Sorbent Doped with $CaCO_3$ for Fast CO_2 Capture in Rapid Intermediate Temperature Swing Sorption. *Chem. Eng. J.* **2018**, *334* (September 2017), 1605–1613.

(37) Jin, S.; Ho, K.; Vu, A.-T.; Lee, C.-H. Salt-Composition-Controlled Precipitation of Triple-Salt-Promoted MgO with Enhanced CO_2 Sorption Rate and Working Capacity. *Energy & Fuels* **2017**, *31* (9), 9725–9735.

(38) Wang, L.; Zhou, Z.; Hu, Y.; Cheng, Z.; Fang, X. Nanosheet MgO-Based CO_2 Sorbent Promoted by Mixed-Alkali-Metal Nitrate and Carbonate: Performance and Mechanism. *Ind. Eng. Chem. Res.* **2017**, *56* (20), 5802–5812.

(39) Ding, J.; Yu, C.; Lu, J.; Wei, X.; Wang, W.; Pan, G. Enhanced CO_2 Adsorption of MgO with Alkali Metal Nitrates and Carbonates. *Appl. Energy* **2020**, *263* (October 2019), 114681.

(40) Hu, Y.; Cui, H.; Cheng, Z.; Zhou, Z. Sorption-Enhanced Water Gas Shift Reaction by in Situ CO_2 Capture on an Alkali Metal Salt-Promoted MgO-$CaCO_3$ Sorbent. *Chem. Eng. J.* **2019**, *377* (August 2018), 119823.

(41) Cui, H.; Zhang, Q.; Hu, Y.; Peng, C.; Fang, X.; Cheng, Z.; Galvita, V. V.; Zhou, Z. Ultrafast and Stable CO_2 Capture Using Alkali Metal Salt-Promoted MgO–$CaCO_3$ Sorbents. *ACS Appl. Mater. Interfaces* **2018**, *10* (24), 20611–20620.

(42) Naeem, M. A.; Armutlulu, A.; Imtiaz, Q.; Donat, F.; Schäublin, R.; Kierzkowska, A.; Müller, C. R. Optimization of the Structural Characteristics of CaO and Its Effective Stabilization Yield High-Capacity CO_2 sorbents. *Nat. Commun.* **2018**, *9* (1), 1–11.

(43) Donat, F.; Müller, C. R. CO_2-Free Conversion of CH_4 to Syngas Using Chemical Looping. *Appl. Catal. B Environ.* **2020**, *278* (July), 119328.

(44) Chen, J.; Shi, T.; Duan, L.; Sun, Z.; Anthony, E. J. Microemulsion-Derived, Nanostructured CaO/CuO Composites with Controllable Particle Grain Size to Enhance Cyclic CO_2 Capture Performance for Combined Ca/Cu Looping Process. *Chem. Eng. J.* **2020**, *393*, 124716.

(45) Donat, F.; Müller, C. R. A Critical Assessment of the Testing Conditions of CaO-Based CO_2 Sorbents. *Chem. Eng. J.* **2018**, *336* (December 2017), 544–549.

(46) Su, C.; Duan, L.; Donat, F.; Anthony, E. J. From Waste to High Value Utilization of Spent

Bleaching Clay in Synthesizing High-Performance Calcium-Based Sorbent for CO_2 Capture. *Appl. Energy* **2018**, *210* (August 2017), 117–126.

(47) Luo, C.; Zheng, Y.; Xu, Y.; Ding, H.; Zheng, C.; Qin, C.; Feng, B. Cyclic CO_2 Capture Characteristics of a Pellet Derived from Sol-Gel CaO Powder with $Ca_{12}Al_{14}O_{33}$ Support. *Korean J. Chem. Eng.* **2015**, *32* (5), 934–938.

(48) Antzara, A. N.; Arregi, A.; Heracleous, E.; Lemonidou, A. A. In-Depth Evaluation of a ZrO_2 Promoted CaO-Based CO_2 Sorbent in Fluidized Bed Reactor Tests. *Chem. Eng. J.* **2018**, *333* (July 2017), 697–711.

(49) Rekhtina, M.; Dal Pozzo, A.; Stoian, D.; Armutlulu, A.; Donat, F.; Blanco, M. V.; Wang, Z.-J.; Willinger, M.-G.; Fedorov, A.; Abdala, P. M.; et al. Effect of Molten Sodium Nitrate on the Decomposition Pathways of Hydrated Magnesium Hydroxycarbonate to Magnesium Oxide Probed by in Situ Total Scattering. *Nanoscale* **2020**, *12* (31), 16462–16473.

(50) Yang, X.; Zhao, L.; Xiao, Y. Effect of $NaNO_3$ on MgO-$CaCO_3$ Absorbent for CO_2 Capture at Warm Temperature. *Energy & Fuels* **2013**, *27* (12), 7645–7653.

(51) Kracek, F. C. The Polymorphism of Potassium Nitrate. *J. Phys. Chem.* **1930**, *34* (2), 225–247.

(52) Chen, J.; Duan, L.; Sun, Z. Accurate Control of Cage-Like CaO Hollow Microspheres for Enhanced CO_2 Capture in Calcium Looping via a Template-Assisted Synthesis Approach. *Environ. Sci. Technol.* **2019**, *53* (4), 2249–2259.

(53) Jansen, D.; Gazzani, M.; Manzolini, G.; Dijk, E. Van; Carbo, M. Pre-Combustion CO_2 Capture. *Int. J. Greenh. Gas Control* **2015**, *40*, 167–187.